Article no. 11

THE CIVIL ENGINEERING JOURNAL 1-2019

WATER HAMMER IN PIPELINE WITH DIFFERENT CHARACTERISTICS OF VALVE CLOSING AND UNSTEADY WALL FRICTION

Haixiao Jing, Wen Wang and Guodong Li

State Key Laboratory of Eco-hydraulics in Northwest Arid Region of China (Xi'an University of Technology), Xi'an, China; jinghx@xaut.edu.cn

ABSTRACT

This paper presents an analytical investigation of water hammer pressure variation in a reservoir-pipe-valve system. Laplace transform method is used to get the analytical solutions for different characteristics of the valve closing. Specifically, sudden valve closing and piecewise linear closing are used, the latter can be treated as approximated arbitrary characteristics of valve closing. Unsteady wall friction is also included. The new solutions compare well with the previous experimental data. The results show that this solution is suitable for water hammer with laminar and low Reynolds number turbulent unsteady flow. The effects of different characteristics of the valve closing on the water hammer pressure variations are also studied. This solution can be a better choice for optimization of valve closing to reduce the maximum water hammer pressure.

KEYWORDS

Water hammer; Laplace transform; Valve closing laws; Unsteady wall friction

INTRODUCTION

Water hammer frequently occurs in pressure pipelines when fluid in motion is forced to stop in a short time. Extreme high and low pressures alter in the process. This phenomenon presents a major problem for practical hydraulic systems, such as bursts of pipe and intrusion of contaminated water. More than 80% of breakdowns in water supply systems can be attributed to water hammer phenomenon [1]. Numerous investigations have been carried out for this problem, which can be traced back to 19th century. Steady state wall friction based on Darcy-Weisbach formula is used widely in classical one dimensional water hammer equations. However, due to the nonlinearity of friction term, numerical methods are applied extensively to solve these equations numerically. While unsteady wall friction is found to be important and two types of unsteady wall friction models are developed. One is the model developed firstly by Zielke [2], in which the unsteady wall friction is represented by a convolution term. The other is the one by Brunone et al.[3] where unsteady wall friction is related to instantaneous mean flow, instantaneous local acceleration and instantaneous convective acceleration. After that, many investigations have been carried out to extend the unsteady friction model to turbulent flow [4]. To get the solution of the water hammer model, most of the studies have focused on the development of numerical models by method of characteristics, such as Bergant et al.[5]. Other numerical methods, such as finite volume method [6] are also used for this problem. Yao et al.[7] investigated the attenuation of water hammer pressure by a time-varying valve closure by multiple scale asymptotic method. Ghidaoui et al.[8] have made good review about the theoretical and practical aspects of water hammer.

An important objective of water hammer analysis is the prediction of water hammer pressure and reduction (or control) of the pressure during water hammer process. Several methods can be used to reduce water hammer pressure, including: 1) optimization of the operation

of the pipe system, 2) modification of existing infrastructure and 3) installation of protection devices, such as relief valve [9]. Previous studies have shown that the pattern of water hammer pressure is strongly dependent on the duration of valve closure and changes of valve operation can reduce water hammer pressure significantly [10]. Azoury et al.[11] studied the effects of valve closure schedule on water hammer by method of characteristics. Provenzano et al.[12] derived analytical solutions for different closing function without considering wall friction.

In recent years, accurate control of water hammer pressure is revisited by optimizing the valve operation using optimization models. Bazargan-Lari et al.[13] optimized closing valve rule curve by using a multi-objective optimization model and Bayesian networks. Chen et al.[14] obtained optimal parameter selection of valve closing using nonlinear optimization techniques. Bohorquez and Saldarriaga [9] proposed a methodology for obtaining the optimal valve closure curves in water distribution systems in Bogota, Colombia. Numerical methods are used to solve water hammer equations in all these optimization studies. While Cao et al.[15] derived a travelling wave solution and solved the extremum of the function by Ritz method to realize the accurate control of water hammer in pipes. However, the wall friction is neglected in their study. Optimal flow control of water hammer requires a forecasting model capable of predicting the non-uniform and unsteady water flow in space and time [14]. Analytical solution is still very useful because it helps to reach clear and in-depth physical understanding and also to provide sufficiently simple yet general and accurate tool for practical prediction and control [16]. However, previous analytical studies of water hammer are confined to sudden valve closing and frictionless pipe.

In this study, analytical solutions for water hammer with unsteady friction and different valve closing laws are derived. Laplace transform method is employed for this purpose. The rest of the paper is structured as follows. Firstly, the governing equations are briefly described and dimensionless variables are introduced. Then, analytical solution for any type of closing valve laws is derived by using Laplace transform. Two special solutions for sudden closing law and piecewise linear closing law are obtained. Unsteady wall friction is then included by following reference [17]. The analytical results are validated by comparing with experimental data. The effects of different closing laws on pressure variations are studied by using the analytical solution. Method of transforming the profile of velocity decrease at valve end to variation of valve opening is also presented. Finally, some conclusions are drawn.

METHODS

Governing equations

A simple reservoir-pipe-valve system is considered in this study, as is shown in Figure 1. After the closing of the valve, the governing equation for the perturbed flow velocity u(x,t) and dynamic pressure $\mathrm{p(x,t)}$ are as follows:

$$\frac{1}{\rho_0 c^2}\frac{\partial p}{\partial t}+\frac{\partial u}{\partial x}=0 \tag{1}$$

$$\frac{\partial u}{\partial t}+\frac{1}{\rho_0}\frac{\partial p}{\partial x}=-\frac{2}{\rho_0 R}\tau_w \tag{2}$$

Where, ρ_0 is the unpertubed fluid density, c is the pressure wave velocity which is dependent on the compressibility of fluid and pipe wall. R is the inner radius of pipe and τ_w denotes the wall shear stress. In the literature of hydraulics, steady state wall friction based on Darcy-weisbach formula is often used [8]. While unsteady wall friction is also proposed and proved to be important for water hammer phenomenon [18].

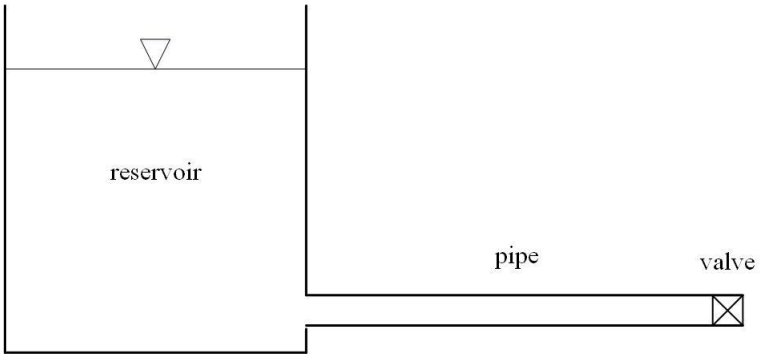

Fig. 1 - Sketch of the pipeline system

Boundary condition (BC) at reservoir end ($x = 0$) is:

$$p(x,t) = 0, \qquad x = 0 \tag{3}$$

This represents the constant pressure head at reservoir. While at valve end ($x = L$), BC becomes

$$u(x,t) = U(t), \qquad x = L \tag{4}$$

Or

$$\frac{\partial p}{\partial x} = -\rho_0 \frac{\partial u}{\partial t} = -\rho_0 \frac{dU}{dt} = f(t), \qquad x = L \tag{5}$$

Where, Equation(2) without wall friction has been used. $U(t)$ represents the valve closing law.

Initial conditions (ICs) for this problem are:

$$p(x,t) = 0, \qquad t = 0 \tag{6}$$

$$\frac{\partial p}{\partial t} = 0, \qquad t = 0 \tag{7}$$

Numerical methods, such as method of characteristics, finite volume method etc., are widely used to solve the above governing equations [5]. In hydraulic engineering, dynamic pressure $p(x,t)$ for water hammer has received more attention. In order to get analytical solution of $p(x,t)$, we will separate the two unknows $u(x,t)$ and $p(x,t)$.

After cross differentiation of Equation (1) and (2), we can eliminate $u(x,t)$ and obtain

$$\frac{\partial^2 p}{\partial x^2} - \frac{1}{c^2}\frac{\partial^2 p}{\partial t^2} = -\frac{2}{R}\frac{\partial \tau_w}{\partial x} \tag{8}$$

This is the governing equation for dynamic pressure $p(x,t)$ of water hammer. The BCs and ICs keep unchanged as above.

For simplicity, dimensionless variables are introduced as in [17]

$$u^* = \frac{u}{U_0}, p^* = \frac{p}{\rho_0 c U_0}, t^* = \frac{t}{L/c}, x^* = \frac{x}{L}, \tau_w^* = \frac{\delta \tau_w}{\rho_0 \nu U_0} \tag{9}$$

Where, * denotes the dimensionless variables, $\delta = \sqrt{\nu L/c}$ is the characteristic thickness of the Stokes oscillatory boundary layer. ν denotes the kinematic viscosity of fluid. Then the dimensionless governing equation for pressure, ICs and BCs become

$$\frac{\partial^2 p^*}{\partial x^{*2}} - \frac{\partial^2 p^*}{\partial t^{*2}} = -\frac{2\delta}{R}\frac{\partial \tau_w^*}{\partial x^*} \tag{10}$$

ICs at $t^* = 0$ become

$$p^*(x^*, t^*) = 0, \qquad \frac{\partial p^*(x^*, t^*)}{\partial t^*} = 0 \tag{11}$$

BCs become

$$p^*\left(x^*,t^*\right)=0, \qquad x^*=0 \tag{12}$$

$$\frac{\partial p^*}{\partial x^*}=-\frac{\partial u^*}{\partial t^*}=f\left(t^*\right), \qquad x^*=1 \tag{13}$$

From now on, * will be omitted for all dimensionless variables for brevity.

Solution by integral transform method for arbitrary closing laws

After neglecting the wall shear stress and taking Laplace transform for the governing equation and BCs, we get:

$$\frac{\partial^2 \bar{p}}{\partial x^2}-s^2\bar{p}=0, \qquad 0<x<1 \tag{14}$$

BCs:

$$\bar{p}=0, \qquad x=0 \tag{15}$$

$$\frac{\partial \bar{p}}{\partial x}=F\left(s\right), \qquad x=1 \tag{16}$$

Where, ICs have been used and

$$\bar{p}\left(x,s\right)=\int_0^\infty e^{-st}p\left(x,t\right)dt, \quad p\left(x,t\right)=\frac{1}{2\pi i}\int_\Gamma e^{st}\bar{p}\left(x,s\right)ds \tag{17}$$

$\mathrm{F}(s)$ is the Laplace transform of $\mathrm{f}(t)$.

The above ordinary differential equation can be easily solved, the solution is:

$$\bar{p}\left(x,s\right)=F\left(s\right)\frac{\sinh\left(sx\right)}{s\cosh\left(s\right)} \tag{18}$$

Define

$$G\left(x,s\right)=\frac{\sinh\left(sx\right)}{s\cosh\left(s\right)} \tag{19}$$

Hence, $\mathrm{p}(x,t)$ can be obtained after inverse Laplace transform

$$\begin{aligned} p\left(x,t\right)&=\frac{1}{2\pi i}\int_\Gamma e^{st}F\left(s\right)G\left(x,s\right)ds \\ &=f\left(t\right)*g\left(t\right)=\int_0^t f\left(t'\right)g\left(t-t'\right)dt' \end{aligned} \tag{20}$$

Where, convolution theorem has been used. $\mathrm{g}(t)$ is the inverse Laplace transform of $\mathrm{G}(s)$ and can be obtained as below.

$$g\left(t\right)=\frac{1}{2\pi i}\int_\Gamma e^{st}G\left(s\right)ds==\frac{1}{2\pi i}\int_\Gamma e^{st}\frac{\sinh\left(sx\right)}{s\cosh\left(s\right)}ds \tag{21}$$

For the integral above, simple poles at:

$$s=i\frac{\left(2m+1\right)\pi}{2}=ik_m, \qquad m=0,\pm1,\pm2,\pm3,\cdots \tag{22}$$

By Cauchy's residue theorem, we get:

$$\begin{aligned} g\left(t\right)&=\sum_{m=-\infty}^{\infty}\frac{e^{ik_mt}}{ik_m}\frac{\sinh\left(ik_mx\right)}{\sinh\left(ik_m\right)}=\sum_{m=-\infty}^{\infty}\frac{1}{ik_m}\frac{\sin\left(k_mx\right)}{\sin\left(k_m\right)}e^{ik_mt} \\ &=\sum_{m=0}^{\infty}\frac{2}{k_m}\frac{\sin\left(k_mx\right)}{\sin\left(k_m\right)}\sin\left(k_mt\right) \end{aligned} \tag{23}$$

Where, $k_{-(m+1)}=-k_m$ has been used.

Finally, for given valve closing law $\mathrm{f}(t)$, we can get $\mathrm{p}(x,t)$ from Equation (20).

Two special closing laws with unsteady friction

From the boundary condition at valve end Equation(5), different $f(t)$ represent different characteristics of valve closing. In this section, two valve closing laws, these are sudden closing and piecewise linear closing, are studied. Also, unsteady friction is included in the results by following [17].

Sudden valve closing

For this case, the dimensionless BC at valve end ($x = 1$) for $u(x,t)$ is

$$u(t) = 1 - H(t) \tag{24}$$

Where, $H(t)$ is Heaviside step function.

Hence, $p(x,t)$ at valve end ($x = 1$) can be obtained

$$\frac{\partial p}{\partial x} = -\frac{\partial u}{\partial t} = \delta(t) \tag{25}$$

Where, $\delta(t)$ is Dirac delta function.

So, we have $f(t) = \delta(t)$. From Equation (20), the pressure p can be calculated:

$$\begin{aligned} p(x,t) &= \int_0^t f(t')\, g(t-t')\, dt' \\ &= \int_0^t \delta(t') \sum_{m=-\infty}^{\infty} \frac{1}{ik_m} \frac{\sin(k_m x)}{\sin(k_m)} e^{ik_m(t-t')} dt' \\ &= \sum_{m=-\infty}^{\infty} \frac{1}{ik_m} \frac{\sin(k_m x)}{\sin(k_m)} \int_0^t \delta(t') e^{ik_m(t-t')} dt' \\ &= \sum_{m=-\infty}^{\infty} \frac{1}{ik_m} \frac{\sin(k_m x)}{\sin(k_m)} e^{ik_m t} \end{aligned} \tag{26}$$

Considering the fact that the time scale of wall friction is much longer than one water hammer pressure cycle, Mei and Jing[17] included unsteady wall friction in their formula by introducing a slow vary parameter $P_m(t)$. $P_m(t)$ can be explicitly expressed by using asymptotic method of multiple scales and boundary layer theory. In this study, unsteady wall friction is included by following exactly the method but not repeat here for simplicity. The final dimensionless result becomes:

$$p(x,t) = \sum_{m=-\infty}^{\infty} P_m(t) e^{ik_m t} \frac{\sin(k_m x)}{ik_m \sin(k_m)} \tag{27}$$

$$P_m(t) = e^{-\lambda_m \varepsilon t}, \qquad \lambda_m = \left(1 + i\,\mathrm{sgn}(k_m)\right)\sqrt{\frac{|k_m|}{2}} \tag{28}$$

And $\mathrm{sgn}(k_m)$ denotes the sign of k_m. $\varepsilon = \delta/R$ is a small dimensionless parameter. δ has been defined in above section.

Piecewise linear valve closing

We can approximate any closing curve by using piecewise linear lines. So dimensionless boundary condition at valve end ($x = 1$) for u becomes:

$$u(t) = \begin{cases} a_1 t + b_1, & t_0 < t < t_1 \\ \cdots & \\ a_n t + b_n, & t_{n-1} < t < t_n \\ \cdots & \\ a_N t + b_N, & t_{N-1} < t < t_N \\ 0, & t > t_N \end{cases} \tag{29}$$

Where, a_n and b_n are coefficients to be determined. And the following constraints must be required.

$$u(t)=\begin{cases}1, & t=0\\ 0, & t=t_c\end{cases} \tag{30}$$

Besides, $u(t)$ must be continuous.

Similarly, BC at valve end for p becomes:

$$\frac{\partial p}{\partial x}=-\sum_{n=1}^{N}a_n\left[H\left(t-t_{n-1}\right)-H\left(t-t_n\right)\right] \tag{31}$$

Hence,

$$f\left(t\right)=-\sum_{n=1}^{N}a_n\left[H\left(t-t_{n-1}\right)-H\left(t-t_n\right)\right] \tag{32}$$

Finally, solution of pressure p becomes:

$$\begin{aligned}p\left(x,t\right)&=\int_0^t f\left(t'\right)g\left(t-t'\right)dt'\\&=\int_0^t(-1)\sum_{n=1}^{N}a_n\left[H\left(t'-t_{n-1}\right)-H\left(t'-t_n\right)\right]\sum_{m=-\infty}^{\infty}\frac{1}{ik_m}\frac{\sin\left(k_m x\right)}{\sin\left(k_m\right)}e^{ik_m\left(t-t'\right)}dt'\\&=-\sum_{m=-\infty}^{\infty}\frac{1}{ik_m}\frac{\sin\left(k_m x\right)}{\sin\left(k_m\right)}\sum_{n=1}^{N}a_n\int_0^t\left[H\left(t'-t_{n-1}\right)-H\left(t'-t_n\right)\right]e^{ik_m\left(t-t'\right)}dt'\\&=-\sum_{m=-\infty}^{\infty}\frac{1}{ik_m}\frac{\sin\left(k_m x\right)}{\sin\left(k_m\right)}e^{ik_m t}\sum_{n=1}^{N}a_n I_{mn}\end{aligned} \tag{33}$$

Where,

$$I_{mn}=\begin{cases}0, & t<t_{n-1}\\ \dfrac{-1}{ik_m}\left[e^{-ik_m t}-e^{-ik_m t_{n-1}}\right], & t_{n-1}<t<t_n\\ \dfrac{-1}{ik_m}\left[e^{-ik_m t_n}-e^{-ik_m t_{n-1}}\right], & t>t_n\end{cases} \tag{34}$$

Similarly, the unsteady wall friction can be included and the final dimensionless form of $p(x,t)$ becomes:

$$\begin{aligned}p\left(x,t\right)&=\int_0^t f\left(t'\right)g\left(t-t'\right)dt'\\&=-\sum_{m=-\infty}^{\infty}e^{-\lambda_m\varepsilon t}e^{ik_m t}\frac{1}{ik_m}\frac{\sin\left(k_m x\right)}{\sin\left(k_m\right)}\sum_{n=1}^{N}a_n I_{mn}\end{aligned} \tag{35}$$

Where, λ_m and ε are the same as in above section.

RESULTS

Validation of unsteady friction with experiments by Bergant et al.

In order to validate the reliability of analytical result for unsteady friction of water hammer, three experimental results by Bergant et al.[18] for laminar and low Reynolds turbulent water hammer flow are used to compare with analytical results. The experimental setup is as follows. A straight long sloping copper pipe with length $L=37.23m$, diameter $d=22.1mm$ is connected with two water tanks at both ends, the pressure head at upstream end is constant $H=32m$ and a fast closing valve at downstream end is installed. The pipe slope is constant at 5.45%. The pressure head at downstream end is changed to achieve required steady velocity or Reynolds number.

Three cases with steady state velocities $U_0 = 0.1, 0.2, 0.3\ m/s$ are carried out. The Reynolds numbers are 1870, 3750, 5600, respectively. Valve closing time $t_c = 0.009s$ for all three cases, which is $t_c^* = t_c c/L = 0.3189$ for dimensionless closing time. Linear closing law will be used in all three cases. Water hammer wave velocity is $c = 1319 m/s$. Pressure variations at two different locations ($x = 0.5$ at the middle section of the pipe and $x = 1$ at valve end) are recorded.

The results can be found in Figures 2, 3 and 4. Good agreement with experimental data can be found in the first several cycles for all three cases. While with the time increases, slight phase advance appears for three cases. Amplitude decay rates for all three cases are also well captured. For quantitative analysis, it is easy to obtain that $t_c < 2L/c$ for all three cases, which means that valve is closed completely before water hammer pressure reflects back to the valve. Hence the maximum pressure head occurs during the first period and the value can be obtained theoretically from Joukowsky's formula, these are 45.45m, 58.89m and 72.34m for three cases (note that the initial pressure head has been added). For case 1, the maximum pressure heads of experimental and analytical results are 46.04m, 45.23m at $x = 0.5$ and 45.84m, 45.29m at $x = 1.0$. For case 2, the maximum pressure heads of experimental and analytical results are 58.59m, 58.47m at $x = 0.5$ and 58.05m, 58.57m at $x = 1.0$. For case 3, the values are 71.55m, 72.48m at $x = 0.5$ and 71.70m, 71.86m at $x = 1.0$. Both experimental and analytical results are very close to the theoretical ones. It can be found that for all the cases the maximum pressure heads of experimental results at valve end ($x = 1.0$) are slightly lower than the values at the middle section($x = 0.5$) due to the line packing effect, while this phenomenon cannot be found from the analytical results. This is due to the fact, that the line packing effect, which can cause slightly rise of maximum pressure, is neglected in the derivation of the analytical solutions.

More importantly, for the phase difference, it can be obtained from case 1 that the times of the last pressure crests (the 9th pressure period) of experimental and analytical results are 0.958s, 0.947s at the middle cross section($x = 0.5$), and 0.911s, 0.905s at $x = 1.0$. The times of phase advance are 0.011s and 0.006s which are 9.7% and 5.3% of the water hammer period ($4L/c$). For case 2, the phase advance are 8.86% and 7.45% of the water hammer period at sections $x = 0.5$ and $x = 1.0$, respectively. And for case 3, the phase advance are 6.95% and 7.01% of the water hammer period at sections $x = 0.5$ and $x = 1.0$, respectively. The reason of this phase advance is probably due to error of the valve closing time. As is found in [19], the phase advance of water hammer pressure can be observed with the decrease of valve closing time. The time of valve closure in the experiments is 0.009s, which is relatively small and measurement error is difficult to avoid.

In general, the accuracy of this analytical solution is acceptable. The unsteady wall friction used in this study is proved to be suitable for water hammer with laminar flow and low Reynolds number turbulent flow, although it is derived from laminar boundary layer theory in [17].

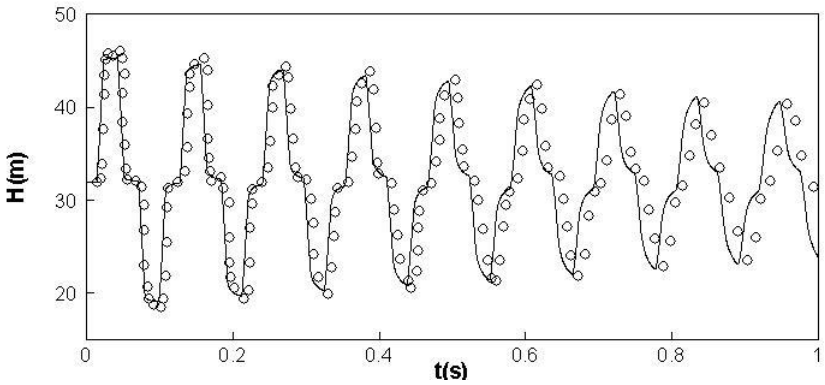

(a) $x = 0.5$

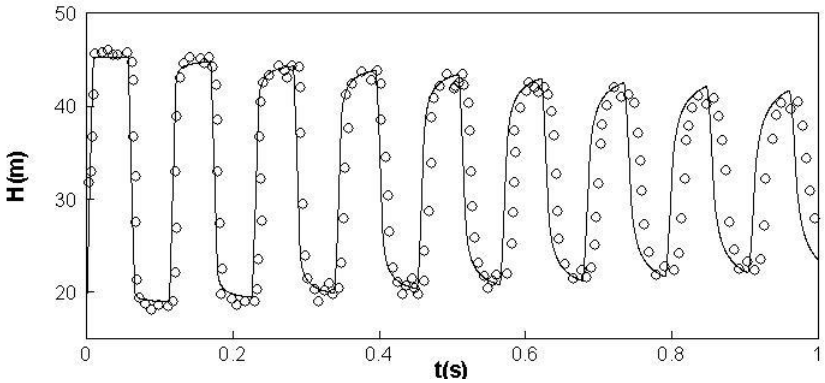

(b) $x = 1.0$

Fig. 2 - Comparison of analytical results with experimental data by Bergant et al.[18] for case 1. Solid lines (analytical results), circles(experimental data).

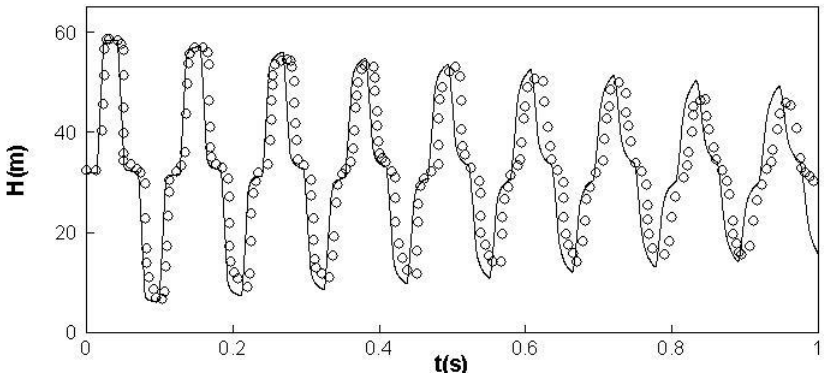

(a) $x = 0.5$

Fig. 3 - Comparison of analytical results with experimental data by Bergant et al.[18] for case 2. Solid lines (analytical results), circles (experimental data).

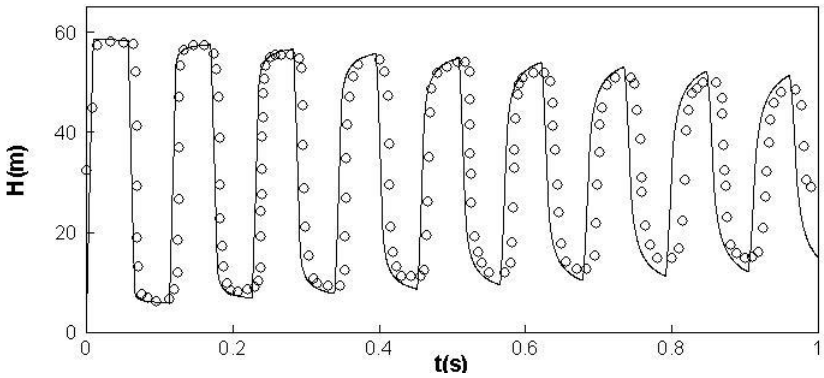

(b) $x = 1.0$

Fig. 3 - Comparison of analytical results with experimental data by Bergant et al.[18] for case 2. Solid lines (analytical results), circles (experimental data).

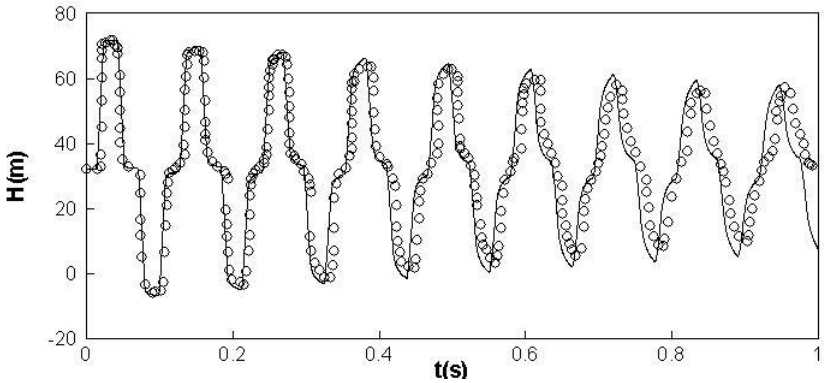

(a) $x = 0.5$

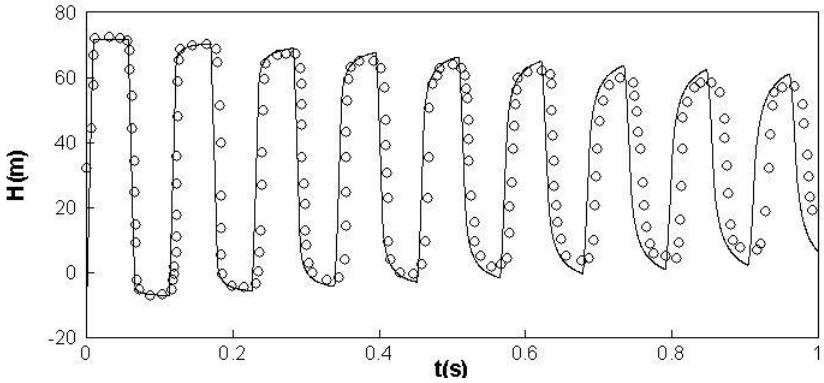

(b) $x = 1.0$

Fig. 4 - Comparison of analytical results with experimental data by Bergant et al.[18] for case 3. Solid lines (analytical results), circles(experimental data).

Effects of valve closing laws on water hammer pressure

There are mainly four types of closing laws for velocity $\mathrm{u}(t)$, including: 1) Convex closing laws; 2)Linear closing law; 3) concave closing laws; 4) sudden closing law. And the following closing function is proposed by Provenzano et al.[12].

$$u(t) = U_0 \left[1 - \left(\frac{t}{t_c} \right)^m \right] \tag{36}$$

Where, m is the exponent. $\mathrm{m} < 1$ is concave closing law, $\mathrm{m} = 1$ is linear closing law and $\mathrm{m} > 1$ is convex closing law. In the following part of this section, dimensionless variables will be used. Figure 5 is the valve closing laws with different exponent m. And $\varepsilon = 0.02$ is used in this case. Different values of dimensionless valve closing time t_c (as is defined in equation (9)) are also chosen to analyse its effects on pressure variations, where the water hammer period is $t_c = 4$ and $t_c = 2$ is the critical value for direct and indirect water hammer.

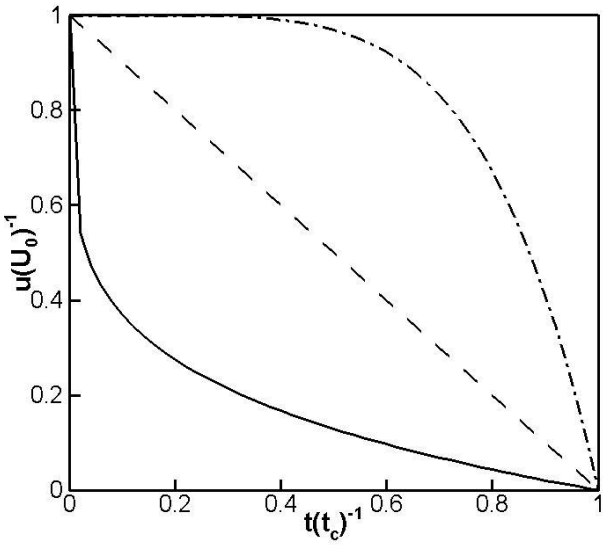

Fig. 5 - Valve closing laws with different exponent m. Solid line($m = 0.2$, dashed line($m = 1$), dash-dot line($m = 5$).

With three closing laws, the results of dimensionless pressure p at valve end($\mathrm{x} = 1$) are given in Figures (6), (7) and (8). From the figures, it can be found that the shapes and amplitudes of pressure vary significantly for different m. For $\mathrm{m} = 0.2$ which represents a fast valve closing followed by a slow valve closing, it can be found from Figure (6) that the pressure increases rapidly then slowly and reaches the maximum value. While for the case $\mathrm{m} = 5$, which represents a slow valve closing followed by a fast valve closing, the water hammer pressure first increases slowly then rapidly, and finally reaches its maximum value. The shapes of the pressure variations are proved to be related to the valve closing laws.

And with the increase of closing time t_c, the maximum amplitudes of the cases with $\mathrm{m} = 0.2$ and $\mathrm{m} = 5.0$ decay slowly. More specifically, the maximum pressures with $\mathrm{t}_c = 1.5$ for both $\mathrm{m} = 0.2$ and $\mathrm{m} = 5.0$ are 1. And when the closing time increases to $\mathrm{t}_c = 4.5$ (note that critical value of valve closing time is $\mathrm{t}_c = 2$), the maximum pressures become 0.849 and 0.894 respectively, with decreases of 15.1% and 10.6%. However, for the case with $\mathrm{m} = 1.0$, the maximum amplitudes become smaller quickly. A decrease of 56.6% is found when closing time increases from $\mathrm{t}_c = 1.5$ to $\mathrm{t}_c = 4.5$. On the other hand, for constant valve closing time the maximum amplitudes of pressure

change obviously with different m. This means that optimization of valve closing laws is an effective way to reduce water hammer pressure.

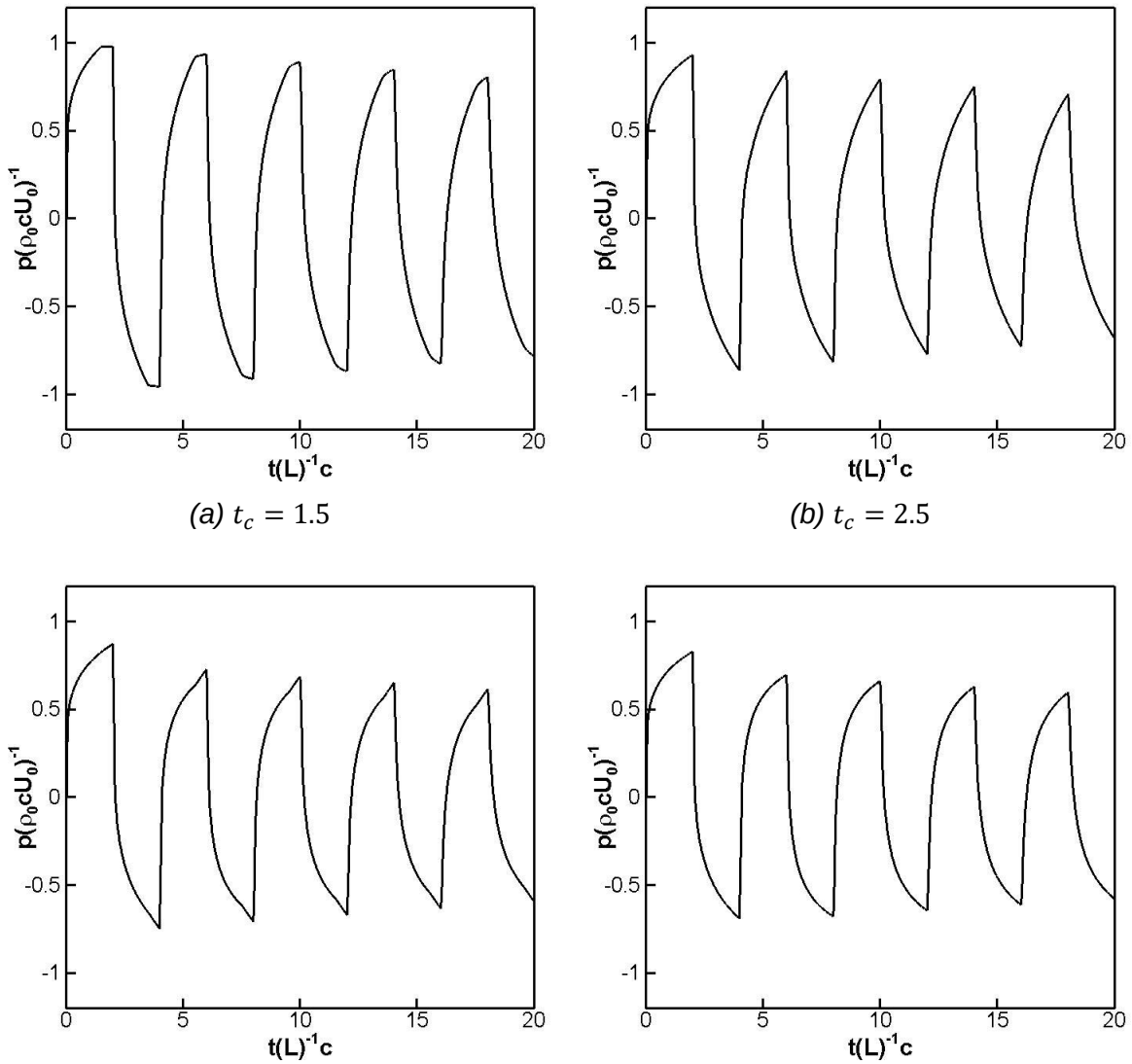

(a) $t_c = 1.5$ (b) $t_c = 2.5$

(c) $t_c = 3.5$ (d) $t_c = 4.5$

Fig. 6 - Pressure p at valve end with $m = 0.2$ and different closing time.

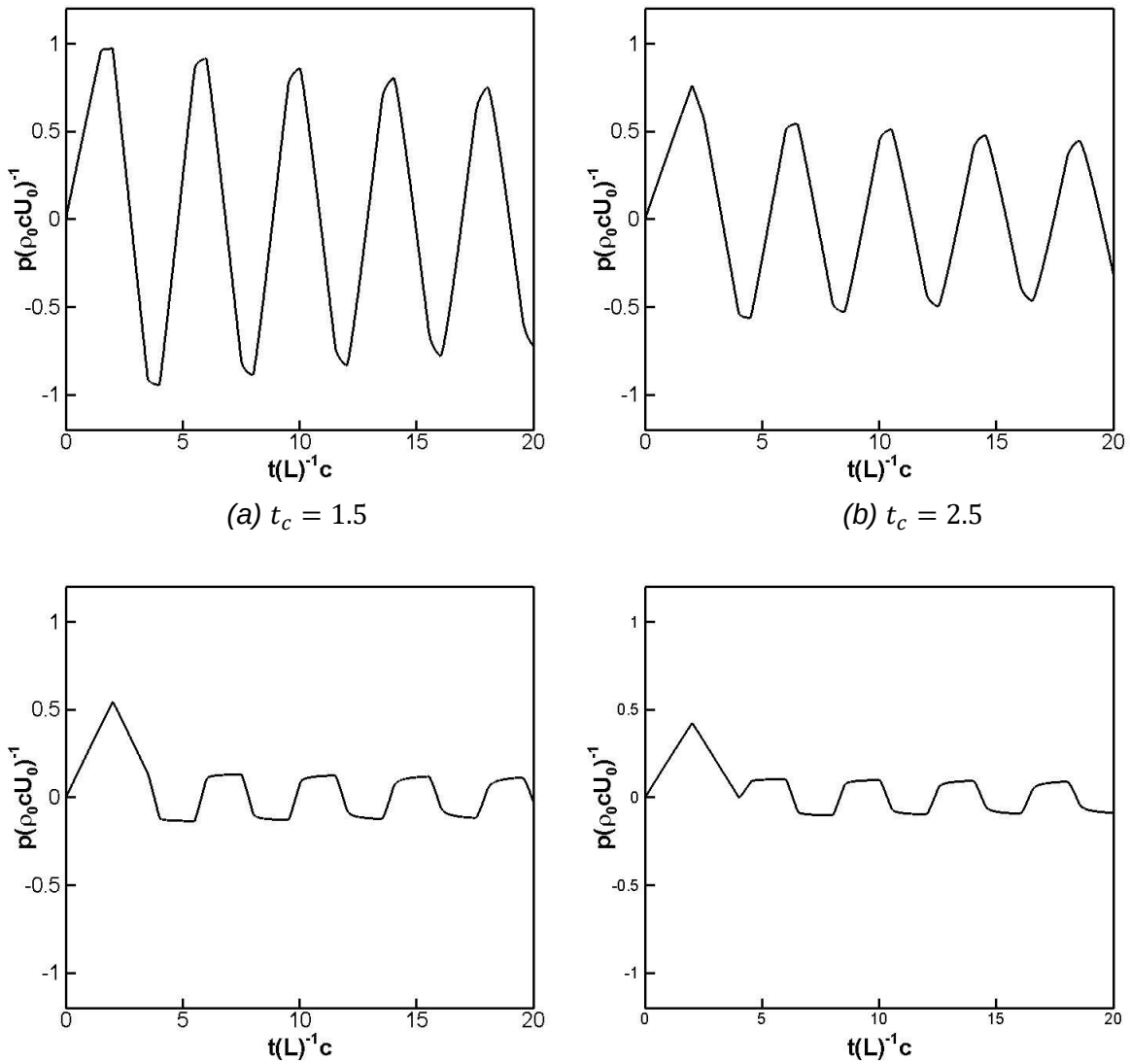

(a) $t_c = 1.5$ (b) $t_c = 2.5$

(c) $t_c = 3.5$ (d) $t_c = 4.5$

Fig. 7 - Pressure p at valve end with $m = 1$ and different closing time.

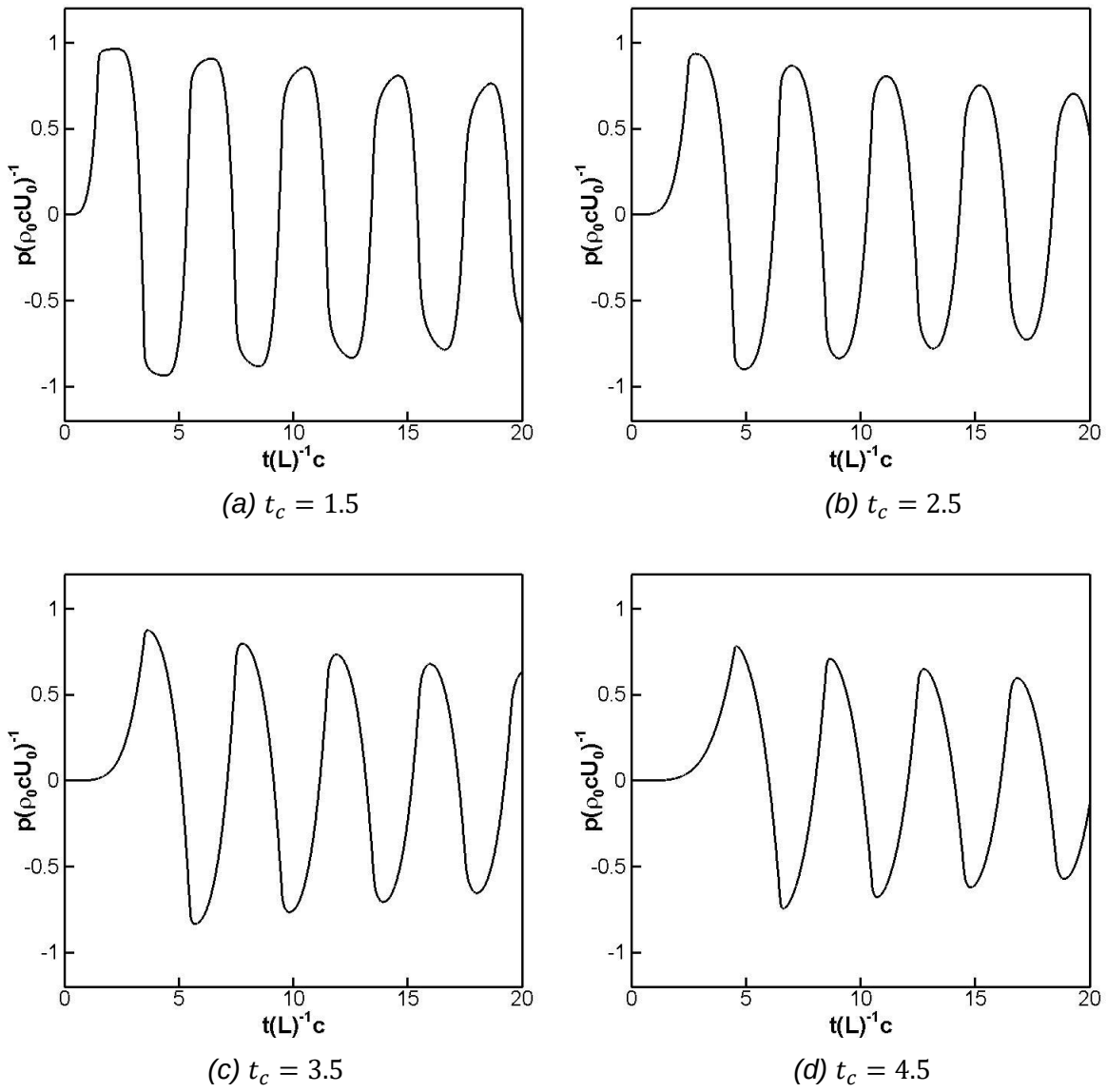

(a) $t_c = 1.5$ (b) $t_c = 2.5$

(c) $t_c = 3.5$ (d) $t_c = 4.5$

Fig. 8 - Pressure p at valve end with $m = 5$ and different closing time.

Relations to the decrease of valve opening

In the above analysis, different schedules of flow velocity variation at valve end are used, however in practical engineering the schedule of valve opening are used and controlled to reduce water hammer pressure. Hence, it is necessary to relate the two ways. At valve end, the pressure head loss and the velocity in dimensional form are related as follows [20].

$$h = \frac{p}{\rho g} = K_L \frac{u^2}{2g}, \qquad x = L \tag{37}$$

Where, K_L is the valve loss coefficient which is dependent on valve type and the valve opening $\kappa = A/A_0$. A is the instantaneous valve opening and A_0 is the area when the valve is fully open. For a given valve and schedule of flow velocity variation at valve end, the schedule of valve opening $\kappa(t)$ can be obtained by combining Equation (37) and (35). Taking a gate valve as example, the relation of loss coefficient K_L and valve opening κ is determined and expressed as follows[21].

$$K_L = \left(\frac{1 + 0.632\sqrt{1-\kappa^2}}{\kappa} - 1 \right)^2 \tag{38}$$

For a linear decrease of flow velocity with different closing time at valve end, the resulted valve opening $\kappa\,(t)$ is presented in Figure 9. It can be found that the linear decrease of flow velocity at valve end indeed does not correspond with a linear closing of the valve. In practical engineering, the optimal velocity variations at valve end can be transformed to the variations of valve opening by this method.

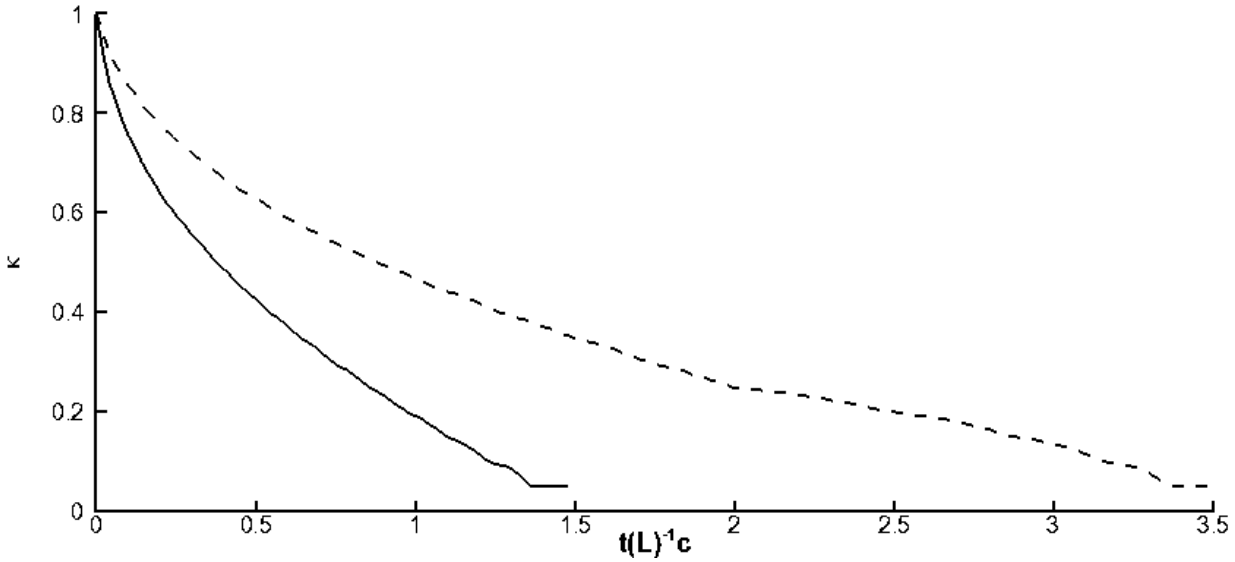

Fig. 9- Variation of valve opening for a linear decrease of flow velocity (gate valve). Solid line: $t_c = 1.5$*, dashed line:* $t_c = 3.5$*.*

CONCLUSION

In this study, a new analytical solution for water hammer in simple reservoir-pipe-valve system is derived by using Laplace transform method. The main differences with previous studies are that both effects of valve closing laws and unsteady wall friction are included in this solution. To validate the solution, experimental data is used by comparing against analytical results of this study. Effects of different valve closing laws on water hammer pressure variations are also studied. Relation of flow velocity decrease at valve end and decrease of valve closing is also proposed. The main conclusions are given as follows.

After comparing with experimental data, the new solution is proved to be suitable for water hammer prediction with initial laminar unsteady flow and low Reynolds number turbulent flow. Comparing the results of three types of closing valve laws, these are convex closing law, linear closing law and concave closing law, the shapes and amplitudes of pressure p at valve end vary obviously. With the increase of closing time, the maximum amplitude of pressure decay faster for linear closing law than that for other two closing laws. And for the same closing time, the maximum amplitudes of different closing laws vary obviously. By using the local head loss formula of valve, it is easy to transform the decrease of flow velocity at valve end to the decrease of valve closing.

In practical hydraulic engineering, the flow is turbulent with high Reynolds number. Analytical solution with unsteady turbulent friction is expected. While analytical solution derived in this paper is still very useful. Firstly, it can be used to validate numerical methods. Secondly, this solution can be employed for the detection of leaks and blockages where the transient flow can be

controlled to be laminar. Besides, for optimization of valve closing laws to control water hammer accurately, this analytical solution is a better choice than the numerical solution.

ACKNOWLEDGEMENTS

This study is supported by the Natural Science Foundation of Education Department of Shaanxi Province, China (No. 16KJ1543).

REFERENCES

[1] Kodura A., 2010. Influence of valve closure characteristic on pressure increase during water hammer run. Environmental engineering III. Taylor & Francis Group, London.
[2] Zielke W., 1968. Frequency-dependent friction in transient pipe flow. Journal of Basic Engineering, vol. 90: 109-115.
[3] Brunone B, Golia UM, Greco M., 1995. The effects of two-dimensionality on pipe transients modeling. Journal of Hydraulic Engineering, vol. 121, no.12: 906−912.
[4] Mitosek M, Szymkiewicz R., 2012. Wave Damping and Smoothing in the Unsteady Pipe Flow. Journal of Hydraulic Engineering, vol. 138, no. 7: 609-628.
[5] Bergant A, Tijsseling AS, Vítkovský JP, et al., 2008. Parameters affecting water-hammer wave attenuation, shape and timing—Part 1: Mathematicaltools. Journal of Hydraulic Research, vol. 46, no.3: 373-381.
[6] Zhao M, Ghidaoui MS., 2004. Godunov-type solutions for water hammer flows. Journal of Hydraulic Engineering, vol. 130, no.4: 341-348.
[7] Yao E, Kember G, Hansen D., 2015. Analysis of water hammer attenuation in applications with varying valve closure times. Journal of Engineering Mechanics, vol.141: 04014107-1.
[8] Ghidaoui MS, Zhao M, Mcinnis DA, Axworthy DH., 2005. A review of water hammer theory and practice. Applied Mechanics Reviews. vol. 58 no.1: 49-76.
[9] Bohorquez J, Saldarriaga J., 2015. Valve operation optimization for minimizing transient flow effects in water distribution systems(WDS). application to main pipes in Bogota, Colombia. World Environmental and Water Resources Congress: Floods, Droughts, and Ecosystems, May 17--21, 2015, Austin.
[10] Streeter VL, Wylie EB.,1967. Hydraulic Transients. McGraw-Hill, New York.
[11] Azoury PH, Baasiri M, Najm H., 1986. Effect of valve-closure schedule on water hammer. Journal of Hydraulic Engineering, vol. 112: 890-903.
[12] Provenzano PG, Baroni F, Aguerre RJ., 2011. The closing function in the waterhammer modeling. Latin American applied research, vol. 41: 43-47.
[13] Bazargan-Lari MR, Kerachian R, Afshar H, Bashi-Azghadi SB., 2013. Developing an optimal valve closing rule curve for real-time pressure control in pipes. Journal of Mechanical Science and Technology, vol. 27: 215-225.
[14] Chen T, Xu C, Ren Z, Loxton R., 2015. Optimal boundary control for water hammer suppression in fluid transmission pipelines. Computers & Mathematics with Applications, vol.69, no.4: 275-290.
[15] Cao HZ, He ZH, He ZY., 2008. The analytical research on the wave process ans optimal control of water hammer in pipes. Engineering Mechanics. Vol. 25, no.6: 22-26.(in Chinese)
[16] Xuan LJ, Mao F, Wu JZ., 2012. Water hammer prediction and control: the Green's function method. Acta Mechanica Sinica, vol.28, no.2: 266-273.
[17] Mei CC, Jing HX. 2016, Pressure and wall shear stress in blood hammer-analytical theory. Mathematical Bioscieces. vol. 280: 62-70.
[18] Bergant A, Simpson AR, Vitkovsky J.,2001. Developments in unsteady pipe flow friction modelling. Journal of Hydraulic Research. vol.39, no.3: 249-257.
[19] Jing HX, Zhang DS, Li GD., 2018. Pressure variations of fluid transients in a pressurized pipeline. Fluid Dynamics Research. Vol. 50: 045514.
[20] Larock BE, Jeppson RW, Watters GZ, 2000. Hydraulics of pipeline systems. CRC Press.
[21] Jović V, 2013. Analysis and modelling of non-steady flow in pipe and channel networks. John Wiley & Sons, Ltd.